

IN-N-OUT: Calibrating Graph Neural Networks for Link Prediction

Erik Nascimento¹, Diego Mesquita², Samuel Kaski^{3,4}, and Amauri H. Souza^{1,3}

¹Federal Institute of Ceará

²Getulio Vargas Foundation

³Aalto University

⁴University of Manchester

Abstract

Deep neural networks are notoriously miscalibrated, i.e., their outputs do not reflect the true probability of the event we aim to predict. While networks for tabular or image data are usually overconfident, recent works have shown that graph neural networks (GNNs) show the opposite behavior for node-level classification. But what happens when we are predicting links? We show that, in this case, GNNs often exhibit a mixed behavior. More specifically, they may be overconfident in negative predictions while being underconfident in positive ones. Based on this observation, we propose **IN-N-OUT**, the first-ever method to calibrate GNNs for link prediction. **IN-N-OUT** is based on two simple intuitions: i) attributing *true/false* labels to an edge while respecting a GNNs prediction should cause but small fluctuations in that edge’s embedding; and, conversely, ii) if we label that same edge contradicting our GNN, embeddings should change more substantially. An extensive experimental campaign shows that **IN-N-OUT** significantly improves the calibration of GNNs in link prediction, consistently outperforming the baselines available — which are not designed for this specific task.

1 Introduction

Graph neural networks [GNNs, 1, 2] are powerful models that often interleave message-passing operators and non-linear activation functions to extract meaningful representations from relational data. These methods have become the *de facto* models for an array of sensitive tasks, including financial crime detection [3], drug discovery [4], personalized medicine [5], and online advertising [6]. As a consequence, domain experts may rely on GNN predictions to make critical decisions. Given the potential risk behind these decisions, there is a growing concern regarding the poor calibration of GNNs — a noticeable mismatch between confidence estimates and true label probabilities. To address this concern, prior works leverage graph structure to improve upon classical calibration methods, either by refining node-wise logits using a GNN [7], or using attention to aggregate logits from nearby nodes and compute node-wise temperature scales [8]. Since these methods operate on node-level logits, they only apply to node classification. However, to the best of our knowledge, there are no works dedicated to the calibration of GNNs for link prediction.

A natural question ensues: *can we use off-the-shelf solutions to calibrate GNNs for link prediction?* In principle, there are many methods designed for independently distributed data that we can use to alleviate miscalibration in GNNs — e.g., isotonic regression [9] and temperature scaling [10]. These methods work directly in logit space, e.g., scaling them by a constant or mapping logits intervals to a sequence of increasing values. The downside of these approaches is that the logits are the final bottleneck in a neural network, and a great deal of information (possibly useful for calibration) may be lost along the way.

In this paper, we propose **IN-N-OUT**, the first method for *post-hoc* calibration of GNNs in the context of link prediction. **IN-N-OUT** is a novel temperature-scaling method that builds on a simple intuition: if a GNN

believes an edge does (not) occur, (not) seeing it should not drastically change the information we have on the graph — which is condensed in the GNN embeddings. On the other hand, if the GNN believes an edge does (not) occur, seeing the opposite should significantly change that edge’s embedding. To encapsulate this concept, IN-N-OUT parameterizes the scaling factor as a function of how much an edge embedding changes by possibly observing an edge, modulated by the class predicted by the GNN.

Our experimental campaign, including multiple datasets and GNN models, shows that IN-N-OUT generally outperforms off-the-shelf calibration methods, consistently resulting in smaller expected calibration errors. More specifically, IN-N-OUT outperforms Isotonic Regression [9], Histogram binning [11], Temperature scaling and BBQ [12], producing lower calibration error on 29 out of 35 experiments. We also run an extensive ablation study with 4 GNNs and 8 datasets to validate the intuitions behind our modeling choices.

In summary, our **contributions** are:

1. We show for the first time that GNNs are usually miscalibrated for link prediction tasks. While this phenomenon also happens for node classification, the calibration curves for link prediction are often more complex, exhibiting a mixed behavior: positive predictions being underconfident, and negative ones being overconfident;
2. We propose IN-N-OUT, the first method for calibration of GNNs in the context of link prediction.
3. Our experiments on real data show that IN-N-OUT consistently outperforms the existing baselines, which include popular calibration methods for non-relational data. We also perform an ablation study to assess the impact of the model components.

2 Background

Notation. We define a graph $\mathcal{G} = (V, E)$, with a set of nodes $V = \{1, \dots, n\}$ and a set of edges $E \subseteq V \times V$. We denote the adjacency matrix of \mathcal{G} by $\mathbf{A} \in \mathbb{R}^{n \times n}$, i.e., A_{ij} is one if $(i, j) \in E$ and zero otherwise. Let \mathbf{D} be the diagonal degree matrix of \mathcal{G} , i.e., $D_{ii} = \sum_j A_{ij}$. We also define the *normalized* adjacency matrix with added self-loops as $\tilde{\mathbf{A}} = (\mathbf{D} + \mathbf{I}_n)^{-1/2}(\mathbf{A} + \mathbf{I}_n)(\mathbf{D} + \mathbf{I}_n)^{-1/2}$, where \mathbf{I}_n is the n -dimensional identity matrix. Furthermore, let $\mathbf{X} \in \mathbb{R}^{n \times d}$ be a matrix of d -dimensional node features. Therefore, throughout this work, we often represent a graph \mathcal{G} using the pair (\mathbf{A}, \mathbf{X}) , where $\mathbf{X} \in \mathbb{R}^{n \times d}$ comprises \mathbf{x}_v in its v -th row. We also denote a node v ’s neighborhood in G by \mathcal{N}_v and its degree by $d_v = |\mathcal{N}_v|$. Furthermore, we use $\{\{\cdot\}\}$ to denote multisets.

Graph neural networks. GNNs are neural networks that exploit a graph’s structure to propagate information between its nodes to create meaningful embeddings, which encapsulate the information regarding their local topologies. One of the most popular ways to see them is through the lens of message-passing [13]. Within this framework, a GNN starts initializing each node’s embedding with its original features, i.e., $\mathbf{h}_v^{(0)} = \mathbf{x}_v$ for all node $v \in V$. At each layer ℓ , in parallel, each node v gathers messages $\mathbf{m}_{u \rightarrow v}^{(\ell)}$ from all its neighbors $u \in \mathcal{N}_v$, compiling them into an aggregated message $\mathbf{m}_v^{(\ell)}$:

$$\mathbf{m}_v^{(\ell)} = \text{Aggregate} \left(\{\{\mathbf{h}_u^{(\ell-1)} : u \in \mathcal{N}_v\}\}\right),$$

where **Aggregate** is a function defined on multisets, i.e., it is order-invariant. Subsequently, each node uses the (so-called) **Update** function to refresh its embedding in light of the aggregated message:

$$\mathbf{h}_v^{(\ell)} = \text{Update} \left(\mathbf{m}_v^{(\ell)}, \mathbf{h}_v^{(\ell-1)} \right).$$

Notably, the majority of GNNs can be described in terms of message-passing by choosing an adequate pair of **Aggregate/Update** functions, modifying G ’s adjacency matrix, or incrementing node features [14]. This is the case for the five GNN architectures we use in our experiments: VGAE, SAGE, PEG, GCN, GIN and SEAL. For instance, VGAE [15] consists of a GCN [16] trained in a variational auto-encoding framework [17]

with a dot product decoder. SAGE [18] is a scalable GNN that randomly subsamples neighbors to speed up message passing, yielding noisy updates. GIN [19] leverages injective aggregate/update functions to boost the expressive power of GNNs. PEG [20] augments node features with a positional embedding, which can capture topological information that cannot be assessed through message-passing alone. SEAL [21] outlines subgraphs to compute edge embeddings via message-passing, further annotating nodes via the *double radius node labeling* trick to increase expressiveness. For a more thorough overview of GNNs, see Hamilton [22].

Link prediction. In the context of link prediction, we can combine node embeddings after an arbitrary number of message-passing layers (say L) to build edge embeddings, which can be fed to an MLP to classify the respective edge. More specifically, we extract build and embedding \mathbf{h}_{uv} for an edge $(u, v) \in V^2$ by applying some function ψ to $\mathbf{h}_u^{(L)}$ and $\mathbf{h}_v^{(L)}$, i.e., $\mathbf{h}_{uv} = \psi(\mathbf{h}_u^{(L)}, \mathbf{h}_v^{(L)})$. When we are dealing with an undirected edge, ψ must also be order-invariant, otherwise, $\mathbf{h}_{uv} \neq \mathbf{h}_{vu}$. In general, we can write the probability for an edge (inferred by a GNN) as $p_{uv} = \text{MLP}(\mathbf{h}_{uv})$. A common metric for evaluating link prediction tasks is hits@k, i.e., % of positive edges receiving higher logits than the negative edge w/ the kth highest logit.

Uncertainty/confidence calibration. Consider a binary classification problem. Let Y and X be the random variables corresponding to the response (binary) variable and the input feature vector. Let also h be a neural network and $h(\mathbf{x}) \in [0, 1]$ be its output probability for the positive class. In this case, $\hat{P} := h(X)$ also characterizes a random variable. We say h is perfectly calibrated if

$$\mathbb{P}(Y = 1 | \hat{P} = c) = c \quad \forall c \in [0, 1]. \quad (1)$$

If we have M input vectors $\mathbf{x}_1, \mathbf{x}_2, \dots, \mathbf{x}_M$ for which h outputs the probability c , Equation 1 entails we expect cM of those vectors to belong to class 1 — and we also expect $(1 - c)M$ to belong to class 0. It is well-known, however, that modern neural networks are poorly calibrated [10]. In the following, we review i) the *expected calibration error*, which is the main metric used to evaluate calibration quality; ii) *reliability diagrams*, which we can use to visually interpret the expected calibration error in deeper detail; and iii) *temperature scaling*, one of the most popular methods for post-hoc calibration of modern neural networks.

The expected calibration error (ECE) measures how far a model is from satisfying Equation 1. To compute the ECE of a binary predictive model h on a sequence of input vectors $\mathbf{x}_1, \dots, \mathbf{x}_M$, we first compute the probabilities $c_1 \dots, c_M$ for class 1, with $c_m := h(\mathbf{x}_m)$. For simplicity of presentation, we define the sequence $(c_1, y_1), \dots, (c_M, y_M)$ of predicted probabilities/true label pairs. Finally, we divide this sequence into N contiguous splits (i.e., ordered bins) B_1, \dots, B_N and compute the ECE as:

$$\text{ECE} = \frac{1}{M} \sum_{n=1}^N \left| \sum_{(c,y) \in B_n} (y - c) \right|. \quad (2)$$

Reliability diagram. Reliability Diagrams are plots that allow for visualizing the calibration as a function of h 's output probability [23]. The diagram comprises a point for each bin B_1, \dots, B_N used to compute the ECE. Each point's horizontal coordinate is the average confidence within that bin, while the vertical one is the frequency of positive labels in that bin. A perfectly calibrated model should lie on the identity line, plotted with the reliability curve for reference.

Temperature-based calibration. The main idea behind temperature-scaling consists of simply scaling all the logits from h by $1/T$ for some $T > 0$. More concretely, suppose we are dealing with a binary classification problem (e.g., link prediction) and let $g(\mathbf{x})$ denote the outputs of h before being projected to the probability simplex (such that $h = \sigma \circ g$). Temperature scaling defines a corrected version of the output as $\hat{h}(\mathbf{x}) = \sigma(g(\mathbf{x}))$ for all input vector \mathbf{x} . Note that when $T \rightarrow \infty$, all predictions tend to $\hat{h}(\mathbf{x}) \rightarrow 1/2$ for any \mathbf{x} . On the other hand, if $T \rightarrow 0$, $g(x) > 0$ implies $\hat{h}(\mathbf{x}) \rightarrow 1$, and $g(x) < 0$ implies $\hat{h}(\mathbf{x}) \rightarrow 0$. Put simply, small T tends to decrease the entropy of our predictive distribution. Conversely, large T tends to flatten our predictive, increasing entropy. In this binary context, temperature scaling can be seen as a special case of Platt's scaling. The main difference between these methods is that the former does not add a bias to the logits — in order

to guarantee h 's accuracy is preserved. Importantly, T is usually learned by minimizing the *negative log likelihood* (NLL) on a labeled validation set, which was not seen during the training of the neural network h .

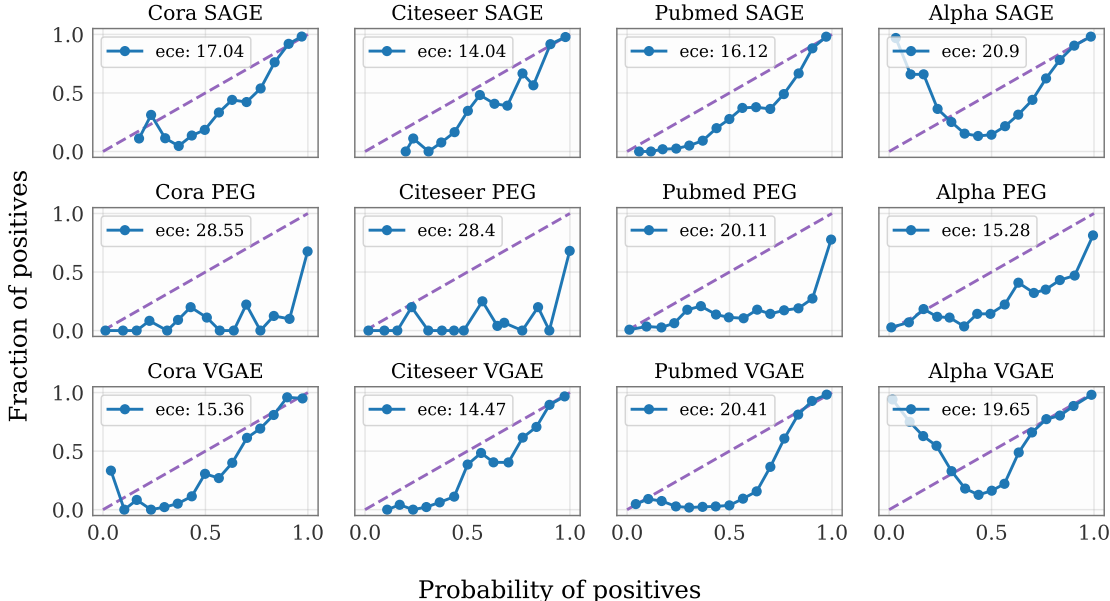


Figure 1: Reliability diagrams of VGAE, PEG and SAGE trained on the cora, citeseer, and pubmed datasets. The dashed line is a baseline for perfect calibration. In most cases, the GNNs tend to attribute higher probability than they should to the positive class. On one hand, this hints at over-confident predictions for edges positively classified. On the other, this indicates under-confidence in our negative predictions. This is behavior is notably more complex than what was previously observed for GNN-based node classification [7, 8], in which predictions are overall underconfident.

3 GNNs’ link predictions are miscalibrated

To assess the extent to which GNNs are miscalibrated, we consider three representative models and four datasets. More specifically, we compute reliability diagrams for PEG, VGAE, and SAGE on the cora, citeseer, pubMed, and bitcoin_alpha datasets [24]. Since we do not aim to benchmark these GNNs, we follow implementation guidelines from the original works, using the same training procedures and hyperparameters whenever available. Appendix A provides further details on implementation and datasets.

Figure 1 shows the reliability diagrams for the representative GNNs. Note that, in most cases, GNNs tend to be overconfident towards the positive class, assigning higher probability to the occurrence of a link than they should. For instance, for pubmed, less than 5% of the links that VGAE predicts with probability $\approx 60\%$ truly occurs. For the cases when the GNNs output probabilities < 0.5 , this means that improving calibration implies increasing the probability for the negative class. Put briefly, GNNs are overconfident when they classify links as positives and underconfident otherwise. This pattern repeats in $\approx 58\%$ of all combinations of dataset/GNN we experimented with. Interestingly, this suggests that GNN-based link prediction results in more complex calibration pattern than observed for both non-relational deep neural networks [10], which are usually overconfident; and GNN-based node classification [7, 8], which are usually underconfident. For completeness, we report reliability diagrams for additional datasets and GNNs architectures in the supplementary material. It is also worth mentioning that the second most common pattern is U-shaped diagrams ($\approx 25\%$), which denote mostly overconfidence in both negative and positive predictions.

4 Calibration using IN-N-OUT

When we are dealing with link prediction, GNNs are usually trained to distinguish nodes that are present in the input graph from spurious ones, created via negative sampling. Typically, we propagate edge embeddings through a feedforward network to compute class probabilities. In this sense, these embeddings summarize all information the GNN deems relevant to infer if the endpoints will connect or not. In summary, the edge embeddings summarize all our knowledge regarding the relationships between the nodes. In light of this intuition, if our GNN points to two nodes connecting with high probability, observing this edge should not change our knowledge about it dramatically, i.e. the edge embedding should not vary substantially. On the other hand, if the GNN outputs a low probability for an edge, seeing it should cause perplexity, substantially changing the corresponding edge embedding. To capture this insight, we propose a temperature scale-based calibration method which we call IN-N-OUT. IN-N-OUT parameterizes the temperature as a function of (a discrepancy between) the embeddings of the edge we want to predict computed with and without that same edge in the input graph.

For concreteness, suppose we want to predict whether an edge (u, v) occurs. Assume further that $A_{uv} = 0$ and let the augmented adjacency matrix \mathbf{A}^+ be defined as:

$$A_{ij}^+ = \begin{cases} A_{ij}, & \text{if } (i, j) \neq (u, v) \\ 1, & \text{otherwise.} \end{cases}$$

Let $\mathbf{H} = \text{GNN}(\mathbf{X}, \mathbf{A})$ such that their u -th row \mathbf{h}_u is the embedding of node u . Following the standard practice from the GNN literature, we define the embedding of an edge (u, v) aggregating the node embeddings \mathbf{h}_u and \mathbf{h}_v using a function ψ , i.e., $\mathbf{h}_{uv} = \psi(\mathbf{h}_u, \mathbf{h}_v)$. In the case where the edge (u, v) is undirected, ψ must be invariant to the order in which node embeddings are given, i.e., $\psi(\mathbf{h}_u, \mathbf{h}_v) = \psi(\mathbf{h}_v, \mathbf{h}_u)$. This order invariance is satisfied, for instance, by the dot product, the average, and the sum operator. To predict the occurrence of an edge (u, v) , we assume that the logit s_{uv} is calculated using an MLP, i.e., $s_{uv} = \text{MLP}(\mathbf{h}_{uv})$.

Then, let $\mathbf{H}^+ = \text{GNN}(\mathbf{X}, \mathbf{A}^+)$ be the node embedding matrix given the incremented adjacency \mathbf{A}^+ . Similarly to what we described earlier for the edge embedding \mathbf{h}_{uv} , let $\mathbf{h}_{uv}^+ = \psi(\mathbf{h}_u^+, \mathbf{h}_v^+)$. Intuitively, when \mathbf{h}_{uv}^+ and \mathbf{h}_{uv} differ (in some sense) by a large margin, adding edge (u, v) conflicts with the previous information that we had on the graph.

In this sense, when our prediction $\hat{y} = \mathbb{1}[s_{uv} > 0]$ is positive, observing a wide margin between \mathbf{h}_{uv}^+ and \mathbf{h}_{uv} should lower our confidence. On the other hand, when $\hat{y} = 0$, the same observation reinforces the notion that the edge (u, v) is *alien* to the graph we are analyzing. Note that this reasoning is in line with the intuition we had regarding Figure 1 — i.e., that the over/under-confidence behavior in link-prediction changes depending on the most-likely class. With that in mind, we propose computing the temperature T_{uv} as a function of a discrepancy measure γ between the embeddings \mathbf{h}_{uv} and \mathbf{h}_{uv}^+ :

$$T_{uv} = \begin{cases} \text{MLP}_{c_1}(\gamma(\mathbf{h}_{uv}, \mathbf{h}_{uv}^+)) & \text{if } s_{uv} > 0 \\ \text{MLP}_{c_2}(\gamma(\mathbf{h}_{uv}, \mathbf{h}_{uv}^+)) & \text{otherwise} \end{cases},$$

where MLP_{c_1} and MLP_{c_2} are multilayer perceptrons (MLPs) used for calibration, and return a scalar $T_{uv} \in \mathbb{R}^+$. To do so, the last layer can be equipped with a non-negative activation function such as the Softplus.

We consider two options for γ : i) the Euclidean distance $\|\mathbf{h}_{uv} - \mathbf{h}_{uv}^+\|_2$, and ii) the difference $\mathbf{h}_{uv} - \mathbf{h}_{uv}^+$ between embeddings after/before edge inclusion. We treat this choice as a hyper-parameter.

To obtain a calibrated probability \hat{p}_{uv} for an edge (u, v) , the *logit* s_{uv} from the original GNN is divided by the temperature T_{uv} and passed through a sigmoid function, so that $\hat{p}_{uv} = \sigma(s_{uv}/T_{uv})$. Importantly, choosing the calibration network (c_1 or c_2) based on s_{uv} 's sign (which encodes whether the prediction is positive/negative) captures well the insight provided in Section 3. More specifically, in the majority of cases, GNN models present opposite calibration behaviors for the positively and negatively predicted links. Nonetheless, our formulation is very general and can accommodate other minority patterns.

Training procedure. To apply IN-N-OUT, we are left with the task of learning MLP_c . We propose doing so by minimizing a conical combination of i) the NLL on a calibration set (\mathcal{L}_{NLL}), comprising positive edges

from the GNN’s training set and negative ones obtained via negative sampling; ii) an ECE term (\mathcal{L}_{ECE}), which directly penalizes miscalibration of our temperature-scaled model; and iii) a penalty term that enforces low confidence on wrong predictions (most likely class \neq ground truth) and high confidence on correct ones (\mathcal{L}_{Cal}). For concreteness, let $\mathcal{C} \subseteq V^2 \times \{0, 1\}$ be our calibration set. More specifically, \mathcal{C} comprises triplets resulting from the concatenation of an edge and its respective label — 1 if observed and 0 if obtained via negative sampling. Then, we can define the negative log-likelihood term as:

$$\mathcal{L}_{\text{NLL}} = \sum_{(u,v,y) \in \mathcal{C}} -y \log(\hat{p}_{uv}) - (1 - y) \log(1 - \hat{p}_{uv}), \quad (3)$$

\mathcal{L}_{ECE} is defined according to Equation 2 using fifteen equally-spaced bins, and we define \mathcal{L}_{Cal} as:

$$\mathcal{L}_{\text{Cal}} = \frac{1}{|\mathcal{C}|} \sum_{(u,v,y) \in \mathcal{C}} -(2y - 1)\hat{p}_{uv} \quad (4)$$

Recall that temperature scaling does not change the most likely classes, so Equation 4 drives the probability \hat{p}_{uv} to 0.5 if the GNN classifies the example incorrectly. Otherwise, if $y = 1$ it pushes \hat{p}_{uv} towards one; and if $y = 0$, it drives \hat{p}_{uv} towards zero. Also, \mathcal{L}_{Cal} can be seen as a simplified version (for binary outcomes) of the calibration penalty proposed by Wang et al. [7] in the context of node classification.

To summarize, our loss function is:

$$\mathcal{L} = \mathcal{L}_{\text{NLL}} + \mathcal{L}_{\text{Cal}} + \lambda \mathcal{L}_{\text{ECE}}, \quad (5)$$

where $\lambda > 0$ is a hyperparameter that we choose by minimizing the ECE in a validation set. It is worth mentioning that we sample negative edges by selecting uniformly at random a pair of nodes for which an edge was not previously observed.

5 Related works

While there are no prior works in the context of link prediction, a few works have tackled the issue for GNN-based node classification. Teixeira et al. [25] first pointed to the issue of miscalibration of GNNs. Wang et al. [7] highlighted an overall underconfident behavior and proposed CaGCN, a method that leverages node embeddings from auxiliary GNN temperature scales, outperforming off-the-shelf calibration strategies. More recently, Hsu et al. [8] further analyzed factors that affect GNN calibration (e.g., diversity of node-wise predictive distributions, and neighborhood similarity) on node classification and devised an attention-based temperature scaling method to address them directly. Wang et al. [26] argued that the shallow nature of GNNs is the culprit behind their underconfidence and proposed counter-acting it using a minimal-entropy regularization term. H. Zargarbashi et al. [27] and Huang et al. [28] proposed methods to compute conformal intervals for GNNs. Furthermore, Vos et al. [29] analyzed the calibration of GNNs within the context of medical imaging tasks.

6 Experiments

In this section, we assess the performance of IN-N-OUT on a variety of datasets and GNNs. Additionally, we run an ablation study to analyze the impact of our design choices on predictive performance. We implemented all experiments using PyTorch [30] and Torch Geometric [31]. Our code is attached as supplementary material.

6.1 Evaluation setup

Datasets. We consider seven real-world datasets for link prediction: Cora, Citeseer, PubMed [32], Twitch, Chameleon [33], Bitcoin-Alpha and Bitcoin-OTC [24, 34]. The first tree datasets are citation graphs in which

Table 1: Expected calibration error (mean and std deviation). The best ECE results found for each GNN are highlighted in blue (the lower the value, the better the model). Notably, IN-N-OUT outperforms the baselines in $\approx 83\%$ of the cases.

	Model	Uncalibrated	Iso	Temp	BBQ	Hist	IN-N-OUT
Cora	VGAE	15.02 \pm 0.76	6.88 \pm 1.72	12.62 \pm 1.79	7.09 \pm 1.09	6.14 \pm 0.76	3.33 \pm 0.67
	SAGE	17.23 \pm 1.74	17.36 \pm 1.84	17.20 \pm 1.47	17.66 \pm 1.10	17.61 \pm 1.19	6.84 \pm 0.48
	PEG	27.91 \pm 0.60	27.65 \pm 1.34	23.90 \pm 1.55	27.30 \pm 1.40	27.43 \pm 1.89	11.53 \pm 1.40
	GIN	15.07 \pm 1.29	16.66 \pm 1.62	14.23 \pm 1.63	16.36 \pm 1.90	16.63 \pm 1.87	4.05 \pm 1.31
	GCN	18.34 \pm 1.13	12.62 \pm 0.97	15.96 \pm 1.11	12.13 \pm 1.30	12.62 \pm 1.08	6.90 \pm 0.79
	SEAL	4.89 \pm 0.18	3.27 \pm 0.15	3.99 \pm 0.66	3.63 \pm 0.24	3.58 \pm 0.20	2.41 \pm 0.36
Cite	VGAE	14.00 \pm 0.67	5.52 \pm 1.81	18.57 \pm 1.86	5.14 \pm 1.29	5.02 \pm 1.36	4.19 \pm 0.65
	SAGE	14.52 \pm 1.89	18.81 \pm 1.14	12.86 \pm 1.56	18.64 \pm 1.90	17.88 \pm 1.82	3.79 \pm 1.98
	PEG	28.39 \pm 1.59	25.15 \pm 1.74	22.30 \pm 1.35	24.82 \pm 1.76	24.93 \pm 0.56	12.02 \pm 0.98
	GIN	15.69 \pm 1.89	23.86 \pm 2.96	13.98 \pm 1.96	23.80 \pm 2.65	23.30 \pm 2.09	2.20 \pm 0.86
	GCN	16.84 \pm 1.62	12.55 \pm 1.43	14.37 \pm 1.19	11.98 \pm 1.59	10.80 \pm 1.62	6.06 \pm 1.23
	SEAL	4.22 \pm 0.31	3.59 \pm 0.49	3.67 \pm 0.35	3.62 \pm 0.30	3.50 \pm 0.24	2.93 \pm 0.28
Pub	VGAE	20.41 \pm 0.64	3.04 \pm 1.52	20.83 \pm 1.86	2.22 \pm 1.59	2.20 \pm 1.97	1.85 \pm 0.37
	SAGE	18.78 \pm 1.42	4.93 \pm 1.41	13.95 \pm 1.72	4.95 \pm 1.57	4.83 \pm 1.32	3.01 \pm 1.32
	PEG	20.49 \pm 1.31	20.31 \pm 1.93	20.34 \pm 1.28	20.22 \pm 0.28	20.00 \pm 1.39	8.21 \pm 0.75
	GIN	15.33 \pm 1.34	12.72 \pm 1.30	14.96 \pm 1.08	12.66 \pm 1.34	12.67 \pm 1.12	3.73 \pm 0.89
	GCN	20.98 \pm 1.79	3.54 \pm 1.97	9.13 \pm 1.97	3.34 \pm 1.68	3.44 \pm 1.75	4.44 \pm 1.46
	SEAL	4.32 \pm 0.33	4.10 \pm 0.17	4.04 \pm 0.16	3.82 \pm 0.48	4.13 \pm 0.32	2.42 \pm 0.34
Twitch	VGAE	16.32 \pm 0.20	1.84 \pm 1.10	16.17 \pm 1.45	1.72 \pm 1.13	1.66 \pm 1.24	1.50 \pm 0.44
	SAGE	16.84 \pm 2.84	2.17 \pm 1.37	23.96 \pm 1.53	2.08 \pm 1.14	1.90 \pm 1.42	1.53 \pm 0.89
	PEG	7.90 \pm 0.91	5.36 \pm 1.19	5.81 \pm 1.19	5.35 \pm 1.11	5.38 \pm 0.09	2.21 \pm 0.51
	GIN	17.86 \pm 2.13	1.91 \pm 0.97	13.78 \pm 2.36	1.85 \pm 0.96	1.86 \pm 0.78	2.69 \pm 0.96
	GCN	16.09 \pm 1.59	2.56 \pm 0.96	6.79 \pm 1.12	1.66 \pm 0.93	1.61 \pm 0.97	4.16 \pm 1.13
	Chame	VGAE	7.52 \pm 1.63	2.83 \pm 1.26	6.39 \pm 1.46	2.84 \pm 1.22	2.77 \pm 1.29
SAGE		5.98 \pm 3.61	3.46 \pm 1.44	12.0 \pm 1.64	3.59 \pm 1.76	3.23 \pm 1.56	2.46 \pm 0.86
PEG		4.44 \pm 0.24	2.84 \pm 0.39	2.28 \pm 0.13	2.82 \pm 0.18	2.44 \pm 0.32	1.66 \pm 0.36
GIN		20.59 \pm 1.96	2.39 \pm 1.23	9.78 \pm 1.08	2.47 \pm 1.17	2.25 \pm 1.31	1.58 \pm 0.97
GCN		26.97 \pm 1.94	1.69 \pm 0.96	12.96 \pm 1.63	1.40 \pm 0.97	1.76 \pm 0.95	3.39 \pm 0.92
SEAL		3.21 \pm 0.49	2.67 \pm 0.33	2.64 \pm 0.29	3.31 \pm 0.26	2.98 \pm 0.22	2.15 \pm 0.32
Alpha	VGAE	20.36 \pm 1.53	9.42 \pm 1.02	10.89 \pm 1.32	8.71 \pm 0.89	8.65 \pm 1.21	8.42 \pm 0.68
	SAGE	21.26 \pm 1.37	13.35 \pm 1.02	12.95 \pm 1.31	13.19 \pm 1.13	13.24 \pm 1.40	6.68 \pm 0.91
	PEG	13.91 \pm 1.13	15.50 \pm 1.09	14.21 \pm 1.16	15.48 \pm 2.02	15.35 \pm 1.03	9.78 \pm 0.89
	GIN	24.32 \pm 2.63	8.89 \pm 1.12	16.93 \pm 1.63	8.84 \pm 1.36	8.80 \pm 1.17	3.32 \pm 0.89
	GCN	20.73 \pm 1.75	6.31 \pm 1.97	9.82 \pm 1.19	6.37 \pm 1.58	6.38 \pm 1.67	6.39 \pm 1.98
	SEAL	2.60 \pm 0.93	3.68 \pm 0.50	3.25 \pm 0.63	3.41 \pm 0.47	3.39 \pm 0.51	2.04 \pm 0.66
OTC	VGAE	18.91 \pm 1.62	6.05 \pm 1.19	6.12 \pm 0.98	5.97 \pm 0.69	5.39 \pm 0.87	9.87 \pm 0.97
	SAGE	24.04 \pm 1.11	13.00 \pm 0.97	14.58 \pm 1.62	12.86 \pm 1.09	12.68 \pm 0.96	15.09 \pm 1.21
	PEG	12.89 \pm 0.86	11.94 \pm 0.99	9.62 \pm 0.86	12.03 \pm 1.01	12.09 \pm 0.95	6.35 \pm 0.95
	GIN	20.01 \pm 1.46	2.55 \pm 0.68	12.96 \pm 1.46	2.08 \pm 0.82	2.02 \pm 0.76	1.23 \pm 0.49
	GCN	20.55 \pm 1.92	5.46 \pm 1.71	10.34 \pm 1.64	5.34 \pm 1.05	5.42 \pm 1.62	4.88 \pm 1.97
	SEAL	2.61 \pm 0.89	3.07 \pm 0.62	3.12 \pm 0.74	2.66 \pm 0.70	2.42 \pm 0.62	2.19 \pm 0.64
DDI	VGAE	9.95 \pm 1.24	5.69 \pm 0.63	5.52 \pm 0.75	5.74 \pm 0.90	5.62 \pm 0.81	4.09 \pm 0.99
	PEG	9.04 \pm 1.16	6.39 \pm 0.22	6.59 \pm 0.71	6.54 \pm 0.53	6.51 \pm 0.42	4.33 \pm 0.48
Collab	VGAE	7.27 \pm 0.73	5.34 \pm 0.43	5.44 \pm 0.52	5.02 \pm 0.49	4.58 \pm 0.62	3.42 \pm 0.58
	PEG	4.73 \pm 0.81	3.11 \pm 0.52	3.08 \pm 0.56	3.94 \pm 0.30	3.57 \pm 0.46	1.42 \pm 0.35

nodes represent documents from different domains, and edges are citation links between these documents. The Twitch dataset comprises attributed graphs where nodes correspond to users, edges denote mutual

friendships, and node attributes encode preferred games, locations, and streaming habits. Chameleon is a network of Wikipedia pages about chameleons. Its nodes represent articles, and edges reflect the mutual links between them. Node features encode the presence of specific nouns in articles and the average monthly traffic from October 2017 to November 2018. Bitcoin-Alpha and Bitcoin-OTC are networks in which nodes correspond to user accounts trading Bitcoin. A directed edge (u, v) denotes the degree of reliability assigned by user u to user v , i.e., each edge has a score denoting the degree of trust. The ogbl-ddi dataset is a homogeneous, unweighted, undirected graph, representing the drug-drug interaction network. The ogbl-collab dataset is an undirected graph, representing a subset of the collaboration network between authors indexed by MAG. Appendix shows summary statistics of the datasets.

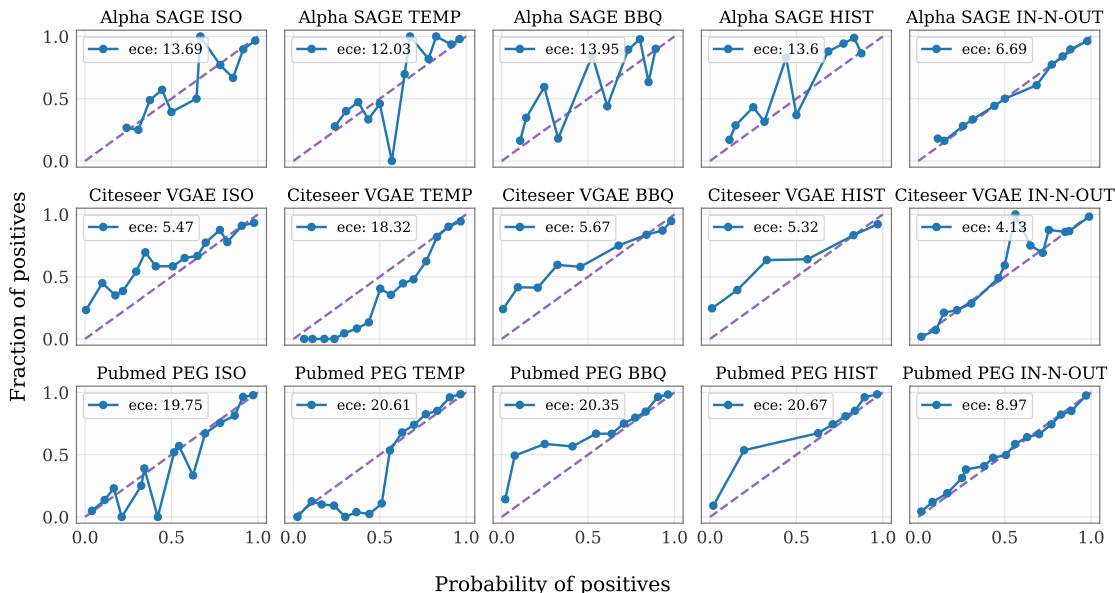


Figure 2: Post-calibration reliability diagrams using IN-N-OUT and off-the-shelf calibration baselines. IN-N-OUT decreases the ECE of the original GNN models and approaches better the identity lines (denoting a perfectly calibrated model).

Baselines. We compare IN-N-OUT to four calibration methods: Isotonic regression [9], Temperature scaling [10], Histogram Binning [11], and Bayesian Binning into Quantiles (BBQ) [12]. We apply these calibration methods to five GNNs: graph sample and aggregate (GraphSAGE) [18], variational graph autoencoder [VGAE, 15], positional-encoding GNN [PEG, 20], graph convolutional networks [GCN, 16], graph isomorphism networks [GIN, 19]. We chose a diverse set of GNNs to allow for a robust assessment, that generalizes beyond specific architectural choices. Rather than benchmarking GNNs on link prediction, we are interested in the calibration aspect of these models. Therefore, we closely follow the original GNNs settings provided in their respective papers. We provide further details in the supplementary material, alongside with the performance of the baseline GNNs on the link prediction datasets.

6.2 Results and Discussion

Table 1 compares the performance of IN-N-OUT against baselines in terms of ECE. Overall, IN-N-OUT is the best-performing method across all datasets and GNNs. More specifically, our method outperforms the baselines in 29/35 (83%) of the experiments — often by a considerable margin. In some scenarios, classic calibration approaches affect negatively the calibration of the baseline (uncalibrated) GNNs. This behavior might be associated to these methods assessing structural information only through logits. For a qualitative assessment, Figure 2 shows the post-calibration confidence diagrams from ISO, TEMP, BBQ,

HIST, and IN-N-OUT on the Citeseer, Pubmed, and Bitcoin-Alpha datasets for the SAGE, VGAE, and PEG models. We observe that, overall, IN-N-OUT better approximates the perfect calibration line compared to the competing methods, which is also reflected in smaller calibration errors (ECE). For instance, note that for the SAGE model trained on Bitcoin-Alpha, predictions produced by IN-N-OUT are well-behaved, mostly following the identity line. On the other hand, competing methods produce an erratic behavior with saw-like patterns.

While classic calibration methods do not impact the accuracy of the underlying GNNs, they might affect other metrics commonly used in link prediction. To assess this effect, Table 2 compares the performance of the methods regarding Hits@20 scores before and after calibration. Due to lack of space in the main manuscript, the supplementary material reports results on additional datasets. Notably, IN-N-OUT has an overall positive effect, sometimes improving Hits@20 scores. On the other hand, using Isotonic Regression, BBQ, and Hist. binning can lead to a significant drop in performance.

Table 2: Hits@20 post-calibration. **Hist** is the most harmful method for this metric while IN-N-OUT improves it in various scenarios. Here we highlight the worst values in red.

Datasets	Model	uncalibrated	Iso	Temp	BBQ	Hist	IN-N-OUT
Cora	SAGE	25.08 ± 1.81	22.46 ± 3.76	25.01 ± 1.81	21.12 ± 2.52	15.42 ± 1.12	26.89 ± 1.19
	PEG	67.32 ± 2.60	51.63 ± 2.34	67.30 ± 2.60	54.01 ± 1.40	51.98 ± 1.89	68.37 ± 1.79
	GIN	52.18 ± 1.16	37.00 ± 1.23	52.18 ± 1.16	30.17 ± 1.30	24.28 ± 1.42	51.23 ± 1.63
Citeseer	SAGE	38.09 ± 2.92	36.73 ± 3.50	38.06 ± 2.92	33.14 ± 4.36	27.98 ± 10.1	40.15 ± 1.59
	PEG	55.11 ± 1.59	53.68 ± 1.74	55.10 ± 1.59	55.16 ± 1.76	53.44 ± 1.56	56.28 ± 1.61
	GIN	38.46 ± 1.86	38.24 ± 1.45	38.46 ± 1.86	32.08 ± 1.23	33.40 ± 1.62	38.45 ± 1.30
Alpha	SAGE	44.97 ± 2.43	39.87 ± 1.34	44.97 ± 2.43	43.48 ± 1.43	37.39 ± 1.13	47.02 ± 1.09
	PEG	49.29 ± 0.89	49.29 ± 0.91	49.29 ± 0.89	49.29 ± 0.96	46.03 ± 1.01	49.29 ± 0.79
	GIN	41.50 ± 1.27	39.73 ± 1.62	41.50 ± 1.27	42.91 ± 1.68	38.17 ± 1.63	45.25 ± 1.40

6.3 Ablation study

To verify that the strategy of comparing edge embeddings with/without the link of interest is crucial to IN-N-OUT’s performance, Table 3 compares it against a simple baseline that computes a temperature scale passing ‘original’ edge embeddings through an MLP (Emb.+MLP). Note that, overall, IN-N-OUT consistently outperforms the baseline.

7 Conclusion

This is the first work on the calibration of GNNs in link prediction tasks. First, we empirically analyzed the confidence prediction patterns for several combinations of GNNs and datasets. We observed that GNNs are often miscalibrated and may depict complex confidence patterns that escape the usual patterns of consistent over- or underconfidence. In particular, the calibration patterns mainly show a dependency on the predicted labels: class-0 predictions tend to be underconfident, whereas class-1 ones are usually overconfident. Based on this insight, we proposed an elegant yet effective temperature-scaling approach for GNNs, called IN-N-OUT. Our method connects this insight with the idea that embeddings carry all the information a model has regarding node relationships — therefore, seeing edges that wildly contradict our predictions should impact embeddings significantly.

Experiments show that IN-N-OUT outperforms classic calibration methods in a combination of 7 datasets and 5 GNNs. By better quantifying uncertainty in GNNs, we believe this works represents an important step towards reliable graph ML methods, with a potential broad impact across diverse application domains.

While our work focused on link prediction, an interesting direction for future work consists of assessing calibration in other tasks like graph classification, temporal link prediction, and dynamic node classification.

Table 3: Expected calibration error (mean and standard deviation). The best ECE results found for each GNN are highlighted in blue. In most cases, IN-N-OUT outperforms the baseline by a considerable margin.

	Model	Uncalibrated	Emb.+MLP	IN-N-OUT
Cite	VGAE	14.00 \pm 0.67	4.92 \pm 1.06	4.19 \pm 0.65
	SAGE	14.52 \pm 1.89	2.62 \pm 0.62	3.79 \pm 1.98
	PEG	28.39 \pm 1.59	17.75 \pm 1.21	12.02 \pm 0.98
Pub	VGAE	20.41 \pm 0.64	3.01 \pm 1.16	1.85 \pm 0.37
	SAGE	18.78 \pm 1.42	4.16 \pm 1.47	3.01 \pm 1.32
	PEG	20.49 \pm 1.31	8.90 \pm 0.89	8.21 \pm 0.75
TW	VGAE	16.32 \pm 0.20	4.81 \pm 1.56	1.50 \pm 0.44
	SAGE	16.84 \pm 2.84	4.06 \pm 1.75	1.53 \pm 0.89
	PEG	7.90 \pm 0.91	2.95 \pm 0.59	2.21 \pm 0.51
Chame	VGAE	7.52 \pm 1.63	3.57 \pm 1.19	1.07 \pm 0.34
	SAGE	5.98 \pm 3.61	3.99 \pm 1.45	2.46 \pm 0.86
	PEG	4.44 \pm 0.24	2.14 \pm 0.21	1.66 \pm 0.36
Alpha	VGAE	20.36 \pm 1.53	7.12 \pm 1.19	8.42 \pm 0.68
	SAGE	21.26 \pm 1.37	7.82 \pm 1.45	6.68 \pm 0.91
	PEG	13.91 \pm 1.13	7.62 \pm 1.76	9.78 \pm 0.89

Acknowledgements

Erik Nascimento was partially supported by the Fundação Cearense de Apoio ao Desenvolvimento Científico e Tecnológico (FUNCAP). Diego Mesquita acknowledges the support by the Silicon Valley Community Foundation (SVCF) through the Ripple impact fund, the Fundação de Amparo à Pesquisa do Estado do Rio de Janeiro (FAPERJ) through the *Jovem Cientista do Nosso Estado* program, the Fundação de Amparo à Pesquisa do Estado de São Paulo (FAPESP) grant 2023/00815-6, and the Conselho Nacional de Desenvolvimento Científico e Tecnológico (CNPq) grant 404336/2023-0. Amauri H. Souza and Samuel Kaski were supported by the Academy of Finland (Flagship programme: Finnish Center for Artificial Intelligence FCAI), EU Horizon 2020 (European Network of AI Excellence Centres ELISE, grant agreement 951847), UKRI Turing AI World-Leading Researcher Fellowship (EP/W002973/1). We also acknowledge the computational resources provided by the Aalto Science-IT Project from Computer Science IT.

References

- [1] F. Scarselli, M. Gori, A. C. Tsoi, M. Hagenbuchner, and G. Monfardini, “The graph neural network model,” *IEEE Transactions on Neural Networks*, 2009.
- [2] M. Gori, G. Monfardini, and F. Scarselli, “A new model for learning in graph domains,” in *IEEE International Joint Conference on Neural Networks (IJCNN)*, 2005.
- [3] D. Cheng, S. Xiang, C. Shang, Y. Zhang, F. Yang, and L. Zhang, “Spatio-temporal attention-based neural network for credit card fraud detection,” *AAAI Conference on Artificial Intelligence*, 2020.
- [4] J. M. Stokes, K. Yang, K. Swanson, W. Jin, A. Cubillos-Ruiz, N. M. Donghia, C. R. MacNair, S. French, L. A. Carfrae, Z. Bloom-Ackermann, V. M. Tran, A. Chiappino-Pepe, A. H. Badran, I. W. Andrews, E. J. Chory, G. M. Church, E. D. Brown, T. S. Jaakkola, R. Barzilay, and J. J. Collins, “A deep learning approach to antibiotic discovery,” *Cell*, vol. 180, no. 4, 2020.

- [5] C. Wu, F. Wu, L. Lyu, T. Qi, Y. Huang, and X. Xie, “A federated graph neural network framework for privacy-preserving personalization,” *Nature Communications*, 2022.
- [6] Z. Liu, B. Ma, Q. Liu, J. Xu, and B. Zheng, “Heterogeneous graph neural networks for large-scale bid keyword matching,” in *ACM International Conference on Information & Knowledge Management (CIKM)*, 2021.
- [7] X. Wang, H. Liu, C. Shi, and C. Yang, “Be confident! towards trustworthy graph neural networks via confidence calibration,” *Advances in Neural Information Processing Systems*, 2021.
- [8] H. H. H. Hsu, Y. Shen, C. Tomani, and D. Cremers, “What makes graph neural networks miscalibrated?” *Advances in Neural Information Processing Systems*, 2022.
- [9] B. Zadrozny and C. Elkan, “Transforming classifier scores into accurate multiclass probability estimates,” in *International Conference on Knowledge Discovery and Data Mining*, 2002.
- [10] C. Guo, G. Pleiss, Y. Sun, and K. Q. Weinberger, “On calibration of modern neural networks,” in *International conference on machine learning*, 2017.
- [11] B. Zadrozny and C. Elkan, “Obtaining calibrated probability estimates from decision trees and naive bayesian classifiers,” in *International Conference on Machine Learning*, 2001, pp. 609–616.
- [12] M. P. Naeni, G. Cooper, and M. Hauskrecht, “Obtaining well calibrated probabilities using bayesian binning,” in *AAAI conference on artificial intelligence*, 2015.
- [13] J. Gilmer, S. Schoenholz, P. Riley, O. Vinyals, and G. Dahl, “Neural message passing for quantum chemistry,” in *International conference on machine learning*, 2017.
- [14] P. Veličković, “Message passing all the way up,” *ArXiv e-prints*, 2022.
- [15] T. N. Kipf and M. Welling, “Variational graph auto-encoders,” *arXiv preprint arXiv:1611.07308*, 2016.
- [16] —, “Semi-supervised classification with graph convolutional networks,” in *International Conference on Learning Representations*, 2017.
- [17] D. Kingma and M. Welling, “Auto-encoding variational Bayes,” *International Conference on Learning Representations*, 2014.
- [18] W. Hamilton, Z. Ying, and J. Leskovec, “Inductive representation learning on large graphs,” *Advances in neural information processing systems*, vol. 30, 2017.
- [19] K. Xu, W. Hu, J. Leskovec, and S. Jegelka, “How powerful are graph neural networks?” *International Conference on Learning Representations*, 2019.
- [20] H. Wang, H. Yin, M. Zhang, and P. Li, “Equivariant and stable positional encoding for more powerful graph neural networks,” in *International Conference on Learning Representations*, 2022.
- [21] M. Zhang and Y. Chen, “Link prediction based on graph neural networks,” *Advances in neural information processing systems*, vol. 31, 2018.
- [22] W. L. Hamilton, “Graph representation learning,” *Synthesis Lectures on Artificial Intelligence and Machine Learning*, vol. 14, no. 3, pp. 1–159, 2020.
- [23] A. Niculescu-Mizil and R. Caruana, “Predicting good probabilities with supervised learning,” in *International Conference on Machine Learning*, 2005.
- [24] S. Kumar, F. Spezzano, V. Subrahmanian, , and C. Faloutsos, “Edge weight prediction in weighted signed networks,” in *International Conference on Data Mining (ICDM)*, 2016.

- [25] L. Teixeira, B. Jalaian, and B. Ribeiro, “Are graph neural networks miscalibrated?” in *Workshop on Learning and Reasoning with Graph-Structured Data*, 2019.
- [26] M. Wang, H. Yang, and Q. Cheng, “Gcl: Graph calibration loss for trustworthy graph neural network,” in *Proceedings of the 30th ACM International Conference on Multimedia*, 2022.
- [27] S. H. Zargarbashi, S. Antonelli, and A. Bojchevski, “Conformal prediction sets for graph neural networks,” in *International Conference on Machine Learning*, 2023.
- [28] K. Huang, Y. Jin, E. Candes, and J. Leskovec, “Uncertainty quantification over graph with conformalized graph neural networks,” *arXiv preprint ArXiv:2305.1435*, 2023.
- [29] I. Vos, I. Bhat, B. Velthuis, Y. Ruigrok, and H. Kuijf, “Calibration techniques for node classification using graph neural networks on medical image data,” in *Medical Imaging with Deep Learning*, 2023.
- [30] A. Paszke, S. Gross, S. Chintala, G. Chanan, E. Yang, Z. DeVito, Z. Lin, A. Desmaison, L. Antiga, and A. Lerer, “Automatic differentiation in pytorch,” in *Advances in Neural Information Processing Systems (NeurIPS - Workshop)*, 2017.
- [31] M. Fey and J. E. Lenssen, “Fast graph representation learning with PyTorch Geometric,” in *Workshop on Representation Learning on Graphs and Manifolds*, 2019.
- [32] P. Sen, G. Namata, M. Bilgic, L. Getoor, B. Galligher, and T. Eliassi-Rad, “Collective classification in network data,” *AI magazine*, vol. 29, no. 3, pp. 93–93, 2008.
- [33] B. Rozemberczki, C. Allen, and R. Sarkar, “Multi-scale attributed node embedding,” *Journal of Complex Networks*, vol. 9, no. 2, 2021.
- [34] S. Kumar, B. Hooi, D. Makhija, M. Kumar, C. Faloutsos, , and V. Subrahmanian, “Rev2: Fraudulent user prediction in rating platforms,” in *International Conference on Web Search and Data Mining*, 2018.
- [35] F. Küppers, J. Kronenberger, A. Shantia, and A. Haselhoff, “Multivariate confidence calibration for object detection,” in *The IEEE/CVF Conference on Computer Vision and Pattern Recognition (CVPR) Workshops*, 2020.

A Datasets and Implementation details

Table 4 shows summary statistics for the datasets used in our experiments. We chose the optimal hyperparameters for all GNNs in this work (see Table 5) using grid search. We consider learning rate values in $\{10^{-1}, 10^{-2}, 10^{-3}\}$, number of epochs in $\{400, 600, 800, 1000\}$ and up to three convolutional layers outputting embeddings of size in $\{16, 32, 64, 128\}$. The embedding size of for the last convolutional layer (out) is chosen independently from the previous layers, which have same dimension (hidden). GCN, GIN, and VGAE use inner products between node embeddings to compute logits for link prediction. SAGE and PEG use a point-wise product of node embeddings followed by a linear layer. We used an 80/10/10% (train/val/test) split for all datasets. For the confidence calibration phase, we train IN-N-OUT using Adam with learning rate 1×10^{-4} with a weight decay 5.0×10^{-8} for 5000 epochs. Similarly to Wang et al. [7] and Hsu et al. [8], we trained all calibrators using the training set partition. We train each GNN (plus dataset) 5 times, and for each time, we calibrate the resulting model 5 times. This adds up to 25 rounds of experiments per dataset/GNN combination. The calibration baselines were implemented with the Netcal package [35]. IN-N-OUT and all GNNs were implemented in Pytorch. We have run all experiments in a computer equipped with a consumer-grade GPU (Nvidia RTX 3060 6GB), an Intel Core i7-12700H 12th generation CPU, and 16GB DDR5 RAM.

Table 4: Summary statistics of the datasets.

Dataset	# Nodes	# Edges	# Feat.	# Labels
Cora	2708	10556	1433	7
PubMed	19717	88648	500	3
Citeseer	3327	9104	3703	6
Twitch	1912	57905	128	2
Chameleon	2277	39730	2325	5
Bitcoin-Alpha	3783	28248	8	2
Bitcoin-OTC	5881	42984	8	2
OGBL-DDI	4267	1334889	5	2
OGBL-Collab	235868	1285465	128	2

Table 5: Optimal hyper-parameters for the GNNs.

Model	hidden	out	layers	lr	epochs
GIN	64	16	2	0.01	1000
SAGE	128	64	2	0.01	1000
VGAE	32	16	2	0.001	400
PEG	20	16	2	0.01	400
GCN	32	16	2	0.001	400
SEAL	32	32	3	0.0001	50

B Time and space complexity of IN-N-OUT

Once IN-N-OUT is trained, its forward pass involves the computation of auxiliary edge embeddings with/without counting edge of interest, as well as a subsequent forward pass of MLP_{c_1} or MLP_{c_2} . That being said, since $\text{MLP}_{c_1}/\text{MLP}_{c_2}$'s are constants in the size of the input graph, IN-N-OUT does not increase the asymptotic time/space complexity of the baseline GNNs.

C Additional results

For each of the 5 GNNs, we run post-hoc calibration 5 times. To confirm the statistical significance of our results, we have run Wilcoxon's signed rank test on the difference between In-N-Out and the second-best calibrator (Table 6) — for cases when In-N-Out is the best calibrator (non-empty entries of Table C). In approximately 80% of the cases, results are statistically significant (denoted by \checkmark).

Table 6: Wilcoxon's sign rank tests $\alpha = 5\%$.

	cora	cite	pub	twitch	chame	alpha	otc
VGAE	\checkmark		\checkmark	\checkmark	\checkmark		
SAGE	\checkmark	\checkmark	\checkmark			\checkmark	
PEG	\checkmark	\checkmark	\checkmark	\checkmark	\checkmark	\checkmark	\checkmark
GIN	\checkmark	\checkmark	\checkmark		\checkmark	\checkmark	\checkmark
GCN	\checkmark	\checkmark					

We report the predictive performance of the GNNs before calibration. Table 7 shows AUC ROC (Area Under the Receiver Operator Characteristic curve), Hits@20, and accuracy values for all GNNs and datasets.

We note that the best-performing method varies with the metric. For instance, on Cora, GCN is the winner if we consider AUC whereas GIN achieves the highest accuracy. On three out of seven datasets, GraphSAGE achieves the lowest average AUC.

Figure 3 shows the reliability diagrams (before calibration) for all GNNs and datasets. Following the trend discussed in the main paper, most diagrams depict a prediction-dependent behavior (overconfident for the positive class and underconfident for the negative one). The second most common pattern represents overconfident predictions for both negative and positive predictions. Moreover, Figure 4 reports post-calibration reliability diagrams. Here, IN-N-OUTS outperforms the baselines with respect to ECE by a large margin in 3 out of 7 datasets.

Table 8 shows Hits@20 values for all models after calibration. Overall, histogram binning achieves the lowest (worst) values, sometimes reaching zero. In such cases, we observe that GNNs assign a probability greater than 0.9 to the twentieth largest negative edge (VGAE does this for Pubmed or Twitch, for example), and these values are within the $(0.9, 1.0]$ bin. As histogram binning collapses the confidence values in a bin to the average of the values in that bin, then Hits@20 will be zero in these cases. Note that this is a behavior that depends on both the GNN and the calibration method.

Table 7: GNN performances prior to calibration (mean and standard deviation for AUC, Hits@20 and ACC).

Dataset	Model	AUC	Hits@20	ACC
cora	VGAE	89.79 ± 0.50	54.70 ± 4.40	74.57 ± 0.76
	SAGE	87.93 ± 1.68	61.48 ± 1.81	75.23 ± 1.74
	PEG	88.01 ± 1.76	61.85 ± 1.38	71.06 ± 1.25
	GIN	89.17 ± 1.54	52.18 ± 1.16	80.64 ± 1.67
	GCN	89.23 ± 1.79	62.80 ± 1.72	78.46 ± 1.85
	SEAL	91.24 ± 0.89	68.29 ± 0.75	79.68 ± 0.83
cite	VGAE	86.36 ± 2.37	50.95 ± 5.21	74.61 ± 0.67
	SAGE	84.89 ± 1.47	56.92 ± 2.92	72.19 ± 1.89
	PEG	90.57 ± 1.62	61.53 ± 2.13	70.65 ± 1.49
	GIN	82.47 ± 1.76	38.46 ± 1.86	78.90 ± 1.81
	GCN	82.24 ± 1.91	58.68 ± 1.10	76.37 ± 1.67
	SEAL	88.06 ± 0.72	67.28 ± 0.91	78.31 ± 0.92
pub	VGAE	95.37 ± 0.37	37.87 ± 2.92	75.49 ± 0.64
	SAGE	89.15 ± 2.28	41.85 ± 1.99	73.68 ± 1.42
	PEG	93.74 ± 2.76	44.35 ± 1.13	77.96 ± 1.34
	GIN	82.50 ± 1.79	26.96 ± 1.24	73.69 ± 1.45
	GCN	84.54 ± 2.16	37.65 ± 2.12	78.65 ± 2.10
	SEAL	96.81 ± 0.26	52.67 ± 0.39	82.97 ± 0.34
Twitch	VGAE	83.70 ± 0.26	19.47 ± 0.24	16.3 ± 0.20
	SAGE	88.03 ± 0.68	20.70 ± 1.41	69.34 ± 0.84
	PEG	91.68 ± 0.72	22.94 ± 1.79	84.69 ± 0.91
	GIN	87.64 ± 1.21	20.96 ± 1.73	65.85 ± 1.12
	GCN	85.49 ± 1.79	24.89 ± 2.03	66.53 ± 2.16
chame	VGAE	97.22 ± 1.17	62.04 ± 2.81	58.70 ± 1.63
	SAGE	53.62 ± 3.31	23.8 ± 0.88	51.62 ± 3.12
	PEG	91.28 ± 0.98	46.67 ± 0.82	75.81 ± 0.97
	GIN	97.06 ± 0.94	71.45 ± 1.08	79.96 ± 0.87
	GCN	87.96 ± 0.76	13.26 ± 1.96	72.16 ± 0.79
	SEAL	98.12 ± 0.54	74.26 ± 0.64	82.13 ± 0.44
alpha	VGAE	81.91 ± 2.21	44.05 ± 2.92	64.37 ± 2.26
	SAGE	75.44 ± 2.14	37.46 ± 1.23	64.02 ± 1.59
	PEG	90.49 ± 1.09	47.87 ± 1.19	82.43 ± 1.07
	GIN	79.15 ± 1.28	41.50 ± 1.27	58.64 ± 1.38
	GCN	86.96 ± 1.81	45.32 ± 1.97	57.60 ± 2.61
	SEAL	93.91 ± 0.41	52.97 ± 0.38	87.28 ± 0.54
OTC	VGAE	82.63 ± 2.76	45.13 ± 2.36	64.02 ± 2.53
	SAGE	79.80 ± 0.87	44.48 ± 0.67	65.65 ± 0.95
	PEG	91.94 ± 1.16	59.56 ± 1.05	83.80 ± 0.76
	GIN	93.00 ± 1.91	46.39 ± 1.98	50.27 ± 1.93
	GCN	88.41 ± 0.94	44.62 ± 1.87	57.60 ± 0.97
	SEAL	95.94 ± 0.61	64.63 ± 0.44	84.34 ± 0.62
DDI	VGAE	76.53 ± 0.28	37.12 ± 0.14	55.27 ± 0.31
	PEG	88.17 ± 0.49	39.07 ± 0.20	62.91 ± 0.49
Collab	VGAE	72.26 ± 0.46	31.14 ± 0.26	46.81 ± 0.44
	PEG	85.57 ± 0.42	34.22 ± 0.30	48.09 ± 0.39

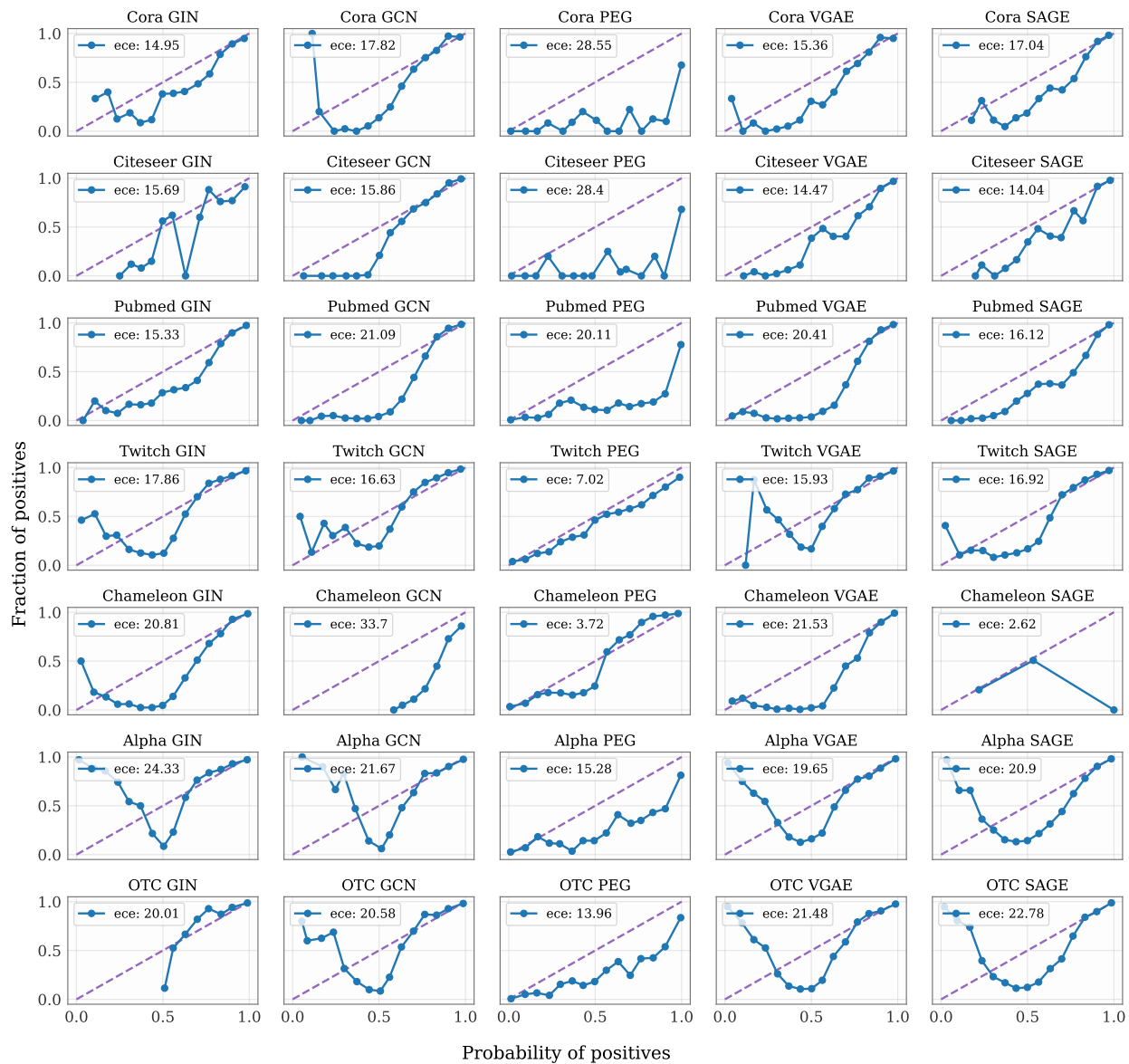


Figure 3: Pre-calibration reliability diagram for all models and datasets.

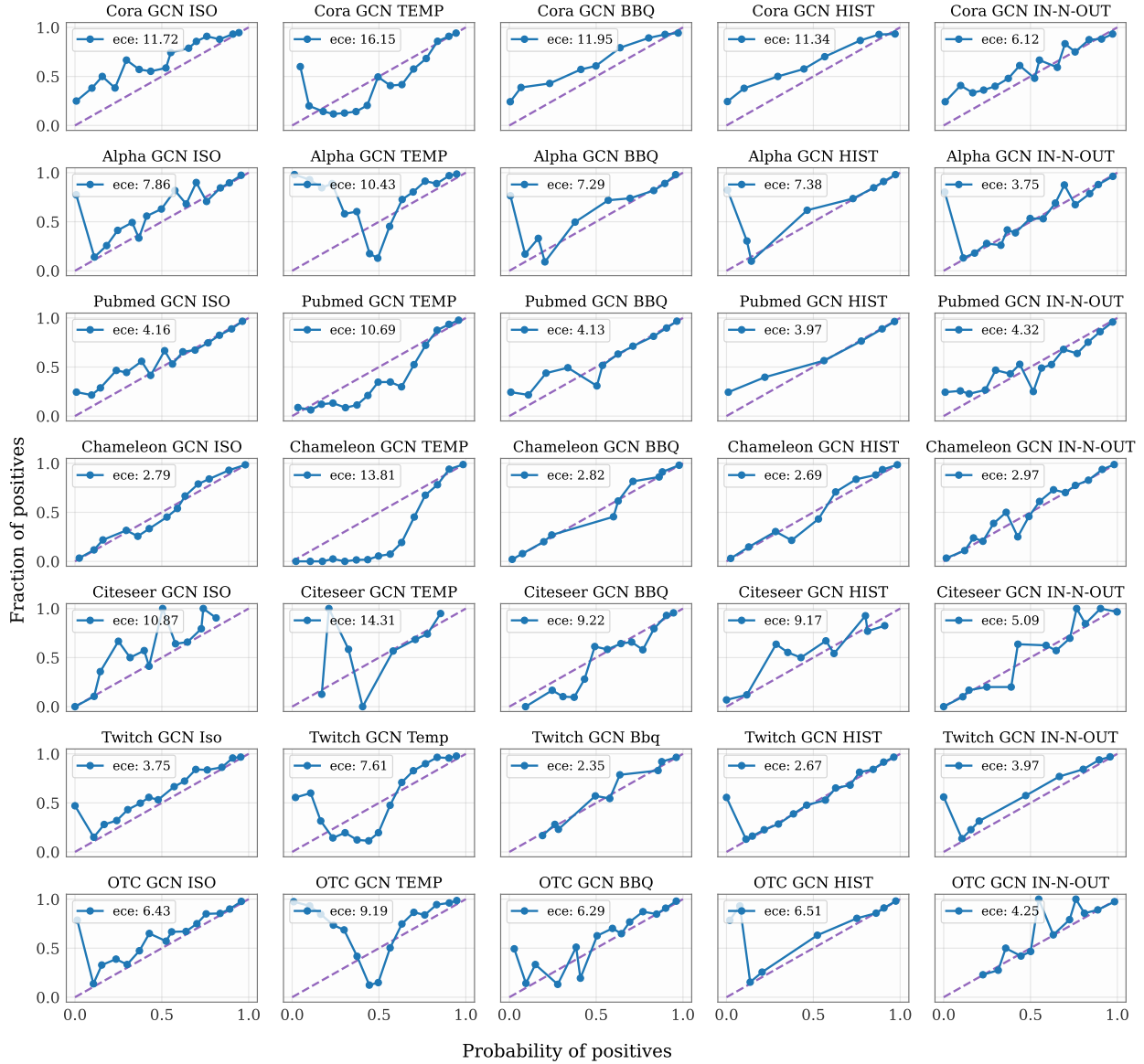


Figure 4: Post calibration reliability diagram for GCN and all datasets. Overall, IN-N-OUT reduced the ECE of all GNNs, resulting in more well-behaved reliability diagrams when compared to [Figure 3](#).

Table 8: Hits@20 post-calibration. The lowest values are highlighted in red. **BBQ** and **Hits** are the most harmful methods for this metric. Importantly, **IN-N-OUT** improves both metrics in most cases ($> 70\%$). Blue denotes cases in which **IN-N-OUT** improves Hits@20.

	Model	uncalibrated	Iso	Temp	BBQ	Hist	IN-N-OUT
cora	VGAE	54.70 \pm 4.40	50.89 \pm 4.27	54.70 \pm 4.40	49.34 \pm 4.67	45.12 \pm 3.94	55.62 \pm 3.15
	SAGE	61.48 \pm 1.81	58.12 \pm 3.76	61.48 \pm 1.81	58.06 \pm 3.71	49.93 \pm 2.76	61.17 \pm 2.72
	PEG	61.85 \pm 1.38	57.21 \pm 2.97	61.85 \pm 1.38	54.78 \pm 2.3	52.98 \pm 1.89	62.39 \pm 2.57
	GIN	52.18 \pm 1.16	37.00 \pm 1.23	52.18 \pm 1.16	30.17 \pm 1.30	24.28 \pm 1.42	51.23 \pm 1.63
	GCN	62.80 \pm 1.72	60.15 \pm 1.92	62.80 \pm 1.72	62.61 \pm 1.69	57.68 \pm 1.39	62.42 \pm 1.21
	SEAL	71.91 \pm 0.92	70.20 \pm 0.98	71.91 \pm 0.92	71.53 \pm 0.85	68.69 \pm 0.89	71.98 \pm 0.80
cite	VGAE	50.95 \pm 5.21	47.98 \pm 4.36	50.95 \pm 5.21	49.79 \pm 4.39	43.18 \pm 4.87	52.15 \pm 3.97
	SAGE	56.92 \pm 2.92	53.97 \pm 2.98	56.92 \pm 2.92	49.53 \pm 4.21	35.75 \pm 4.13	56.89 \pm 2.13
	PEG	61.53 \pm 2.13	56.11 \pm 3.27	61.53 \pm 2.13	53.23 \pm 2.61	51.14 \pm 2.48	62.20 \pm 2.09
	GIN	38.46 \pm 1.86	38.24 \pm 1.45	38.46 \pm 1.86	32.08 \pm 1.23	33.40 \pm 1.62	38.47 \pm 1.30
	GCN	58.68 \pm 1.10	58.24 \pm 1.60	58.68 \pm 1.10	57.14 \pm 1.25	47.47 \pm 1.62	60.21 \pm 1.58
	SEAL	72.48 \pm 0.68	72.48 \pm 0.71	72.48 \pm 0.68	71.72 \pm 0.93	70.96 \pm 0.67	72.48 \pm 0.63
pub	VGAE	37.87 \pm 2.92	37.66 \pm 2.54	37.87 \pm 2.92	35.76 \pm 2.27	0.00 \pm 0.00	38.12 \pm 2.25
	SAGE	41.85 \pm 1.99	39.79 \pm 3.41	41.85 \pm 1.99	25.76 \pm 3.70	23.86 \pm 4.10	41.97 \pm 2.34
	PEG	44.35 \pm 1.13	42.76 \pm 3.89	44.35 \pm 1.13	41.09 \pm 2.73	0.00 \pm 0.00	45.35 \pm 3.02
	GIN	26.96 \pm 1.24	23.87 \pm 1.62	26.96 \pm 1.24	0.00 \pm 0.00	0.00 \pm 0.00	26.92 \pm 1.63
	GCN	37.65 \pm 2.12	34.83 \pm 1.64	37.65 \pm 2.12	28.97 \pm 1.96	0.00 \pm 0.00	38.19 \pm 1.35
	SEAL	72.48 \pm 0.64	72.48 \pm 0.68	72.48 \pm 0.64	70.96 \pm 0.63	70.96 \pm 0.77	72.48 \pm 0.62
Twitch	VGAE	19.47 \pm 0.24	13.50 \pm 0.21	19.42 \pm 0.24	0.04 \pm 0.00	0.04 \pm 0.00	19.66 \pm 1.12
	SAGE	20.70 \pm 1.41	9.49 \pm 2.18	20.70 \pm 1.41	0.00 \pm 0.00	0.00 \pm 0.00	20.28 \pm 1.14
	PEG	22.94 \pm 1.79	21.72 \pm 1.34	22.94 \pm 1.79	0.00 \pm 0.00	0.00 \pm 0.00	22.21 \pm 2.32
	GIN	20.96 \pm 1.73	18.66 \pm 1.53	20.96 \pm 1.73	20.54 \pm 1.42	0.00 \pm 0.00	21.09 \pm 1.50
	GCN	24.89 \pm 2.03	23.45 \pm 1.43	24.89 \pm 2.03	23.64 \pm 1.19	24.16 \pm 1.26	24.80 \pm 1.09
chame	VGAE	62.04 \pm 2.81	52.73 \pm 8.91	62.02 \pm 2.81	0.00 \pm 0.00	0.00 \pm 0.00	64.09 \pm 1.01
	SAGE	23.83 \pm 0.88	19.14 \pm 2.40	23.80 \pm 0.88	22.07 \pm 2.63	22.26 \pm 3.05	23.63 \pm 1.20
	PEG	46.67 \pm 0.82	45.96 \pm 1.58	46.67 \pm 0.82	42.73 \pm 2.03	42.87 \pm 1.90	47.23 \pm 2.34
	GIN	71.45 \pm 1.08	68.33 \pm 1.34	71.45 \pm 1.08	71.24 \pm 1.97	65.63 \pm 1.72	72.56 \pm 1.25
	GCN	13.26 \pm 1.96	11.03 \pm 1.57	13.26 \pm 1.96	0.00 \pm 0.00	0.00 \pm 0.00	13.25 \pm 1.09
	SEAL	74.26 \pm 0.64	74.23 \pm 0.49	74.26 \pm 0.64	70.13 \pm 0.12	69.78 \pm 0.19	74.26 \pm 0.53
Alpha	VGAE	44.05 \pm 2.92	44.01 \pm 3.41	44.05 \pm 2.92	40.91 \pm 2.72	0.00 \pm 0.00	44.96 \pm 2.19
	SAGE	37.46 \pm 1.23	35.18 \pm 2.16	37.46 \pm 1.23	34.76 \pm 2.63	21.34 \pm 2.34	38.06 \pm 1.67
	PEG	47.87 \pm 1.19	43.51 \pm 2.52	47.87 \pm 1.19	44.36 \pm 2.14	34.72 \pm 2.63	47.89 \pm 1.86
	GIN	41.50 \pm 1.27	39.73 \pm 1.62	41.50 \pm 1.27	42.91 \pm 1.68	38.17 \pm 1.63	45.25 \pm 1.40
	GCN	45.32 \pm 1.97	44.33 \pm 1.92	45.32 \pm 1.97	44.61 \pm 1.92	39.02 \pm 1.87	45.49 \pm 1.93
	SEAL	52.97 \pm 0.66	50.63 \pm 0.45	52.97 \pm 0.66	47.73 \pm 0.61	52.19 \pm 0.33	52.97 \pm 0.5
OTC	VGAE	45.13 \pm 2.36	44.97 \pm 3.10	45.13 \pm 2.36	44.16 \pm 2.75	40.03 \pm 1.97	45.35 \pm 2.61
	SAGE	44.48 \pm 0.67	42.09 \pm 2.19	44.48 \pm 0.67	35.91 \pm 1.89	0.00 \pm 0.00	44.52 \pm 1.09
	PEG	59.56 \pm 1.05	54.95 \pm 0.96	59.56 \pm 1.05	53.09 \pm 1.06	52.09 \pm 1.15	59.62 \pm 1.09
	GIN	46.39 \pm 1.98	45.78 \pm 1.82	46.39 \pm 1.98	45.18 \pm 1.59	41.46 \pm 1.57	48.67 \pm 1.47
	GCN	44.62 \pm 1.87	42.34 \pm 1.69	44.62 \pm 1.87	43.92 \pm 1.69	39.92 \pm 1.67	44.98 \pm 1.98
	SEAL	64.32 \pm 0.57	63.94 \pm 0.41	64.32 \pm 0.57	64.32 \pm 0.48	62.42 \pm 0.86	64.33 \pm 0.43
DDI	VGAE	37.12 \pm 0.14	35.16 \pm 0.20	37.12 \pm 0.14	36.19 \pm 0.22	33.26 \pm 0.29	38.97 \pm 0.37
	PEG	39.07 \pm 0.20	38.55 \pm 0.47	39.07 \pm 0.20	37.19 \pm 0.51	34.04 \pm 0.35	39.21 \pm 0.38
Collab	VGAE	31.14 \pm 0.26	31.14 \pm 0.29	31.14 \pm 0.26	31.09 \pm 0.32	28.15 \pm 0.34	31.14 \pm 0.25
	PEG	34.22 \pm 0.30	32.11 \pm 0.65	34.22 \pm 0.30	32.59 \pm 0.51	30.72 \pm 0.24	34.50 \pm 0.63